

Rapamycin inhibits polyglutamine aggregation independently of autophagy by reducing protein synthesis

Matthew A. King, Sarah Hands, Farida Hafiz, Noboru Mizushima, Aviva M. Tolkovsky and Andreas Wyttenbach

Department of Biochemistry, University of Cambridge, Tennis Court Road, Cambridge, CB2 1QW, UK (MAK, FH, AMT, AW); Department of Physiology and Cell Biology, Tokyo Medical and Dental University, 1-5-45 Yushima, Bunkyo-ku, Tokyo 113-8519, Japan (NM); School of Biological Sciences, Neuroscience Group, University of Southampton Bassett Crescent East, Southampton, SO16 7PX, UK (SH, AW)

Running title

Autophagy-independent polyQ aggregation suppression by rapamycin

Correspondence

Andreas Wytenbach, Southampton Neuroscience Group, School of Biological Sciences, University of Southampton. Bassett Crescent East, Southampton SO16 7PX, UK; Tel 0044(0)23-8059-5998; Fax: 0044(0)23-8059-4459 email: aw3@soton.ac.uk

Number of text pages	31
Number of tables	0
Number of figures	8
Number of references	40
Number of words abstract	234
Number of words Introduction	736
Number of words Discussion	1417

Abbreviations

CHX, cycloheximide; EGFP, enhanced green fluorescent protein; Ex1htt, huntingtin exon 1; HD, Huntington's Disease; IB, inclusion body; MEF, mouse embryonic fibroblast; mRFP, monomeric red fluorescent protein; polyQ, polyglutamine

ABSTRACT

Accumulation of misfolded proteins and protein assemblies is associated with neuronal dysfunction and death in several neurodegenerative diseases such as Alzheimer's, Parkinson's and Huntington's Disease (HD). It is therefore critical to understand the molecular mechanisms of drugs that act on pathways that modulate misfolding and/or aggregation. Importantly, the mTOR (mammalian target of rapamycin) inhibitor rapamycin or its analogues have been proposed as promising therapeutic compounds clearing toxic protein assemblies in these diseases via activation of autophagy. However, using a cellular model of HD we found that rapamycin significantly decreased aggregation-prone polyglutamine (polyQ) expanded huntingtin and its inclusion bodies (IB) in both autophagy-proficient and autophagy-deficient cells (by genetic knockout of the *atg5* gene in mouse embryonic fibroblasts). This result suggests that rapamycin modulates the levels of misfolded polyQ proteins via pathways other than autophagy. We show that rapamycin reduces the amount of soluble polyQ protein via a modest inhibition of protein synthesis that in turn significantly reduces the formation of insoluble polyQ protein and IB formation. Hence, a modest reduction in huntingtin synthesis by rapamycin may lead to a substantial decrease in the probability of reaching the critical concentration required for a nucleation event and subsequent toxic polyQ aggregation. Thus, in addition to its previously proposed beneficial effect of reducing polyQ aggregation/toxicity via autophagic pathways, rapamycin may alleviate polyQ disease pathology via its effect on global protein synthesis. This finding may have important therapeutic implications.

The polyglutamine/CAG disorders comprise a group of neurodegenerative diseases that are associated with polyglutamine (polyQ) expansion mutations in the respective disease genes that are otherwise unrelated (Cummings and Zoghbi, 2000). Abnormally long polyQ stretches cause proteins to misfold and produce intracellular protein aggregates. It is thought that polyQ aggregation follows a stochastic nucleation dependent process that initiates oligomerisation, amyloid-like fibril formation and the production of structures called inclusion bodies (IBs) (Perutz and Windle, 2001). Because polyQ misfolding/aggregation is associated with cellular toxicity (Ross and Poirier, 2004), it is crucial to understand the cellular mechanisms that control misfolding/aggregation with a view to the development of drugs that modify these pathways and alleviate disease.

The accumulation of intracellular IBs points to the inability of cells to dispose of mutant polyQ proteins using chaperone-assisted refolding (Muchowski and Wacker, 2005) and proteasome-mediated degradation (reviewed in Jana and Nukina, 2003). Deciphering the mechanisms of degradation and clearance of polyQ expanded proteins, and how such mechanisms might be targeted using drugs, is a major focus of current research. Macroautophagy (here referred to as autophagy) is a process alternative to that of proteasomal degradation by which some long-lived proteins and organelles are cleared (Shintani and Klionsky, 2004). Autophagy may be responsible for clearing polyQ expanded proteins and their assemblies (reviewed in Rubinsztein 2006). Clearance by autophagy occurs by sequestration of the target organelle/protein into double membrane structures called autophagosomes that fuse with endo/lysosomes and discharge their contents, which are subsequently degraded. The mammalian homologue of Atg8 MAP-LC3 (LC3), is a key mediator of autophagy: after LC3 is C-terminally cleaved (LC3 I) phosphatidylethanolamine is added to the C-terminal glycine by the Atg5/12 complex, generating LC3 II bound to the nascent autophagosomal membrane (reviewed in Tanida et al. 2004b). Because the Atg5/12 complex catalytically activates the lipidation of LC3, trace amounts of Atg5 can support substantial autophagy whereas Atg5 knockout cells are totally deficient in autophagy (Hosokawa et al., 2006). The hallmark of autophagic activation is the formation of autophagosome puncta containing LC3 II, while the biochemical measurement of autophagic activity is expressed as the amount of LC3 II that accumulates in the absence or presence of lysosomal activity.

Autophagy was first implicated in the regulation of IB formation and clearance of aggregate-prone proteins based on use of chemical activators/inhibitors including the pro-autophagic drug rapamycin and knockdown of different autophagic genes (see Rubinsztein, 2006 and references therein). The finding that rapamycin and its analogue CCI-779 protect against neurodegeneration in animal

models of misfolding diseases (Ravikumar et al., 2004; Berger et al., 2006) opens up immense hopes for treating debilitating diseases such as the polyQ disorders. Rapamycin, a macrolytic lactone produced by *Streptomyces hygroscopicus*, has immunosuppressive, antimicrobial, and antitumor properties. It binds intracellularly to FK506 binding protein 12 and targets the protein kinase mTOR (mammalian target of rapamycin). Inhibition of phosphorylation of mTOR by rapamycin activates autophagy and it has been suggested that rapamycin (or analogues) ameliorates neurodegenerative proteinopathies via activation of autophagy (reviewed in Rubinsztein, 2006). However, mTOR impacts on various downstream targets not necessarily involved in autophagy, including the control of protein synthesis (reviewed in Dann and Thomas, 2006; Wullschleger et al., 2006) and because of these effects it is currently being evaluated in several Phase II clinical trials for cancer (reviewed in Sabbatini, 2006). It is therefore unclear whether rapamycin mediates its protective effects solely via autophagy.

In order to probe the actions of rapamycin on the formation and clearance of expanded polyQ proteins and IBs we have taken advantage of clonal cell lines of autophagy proficient (Atg5^{+/+}) and deficient (Atg5^{-/-}) mouse embryonic fibroblasts (MEFs) that are easily amenable to biochemical and genetic rescue experiments. Using exon 1 of human htt containing 97 glutamines and fused to EGFP (Ex1HttQ97-EGFP) as an aggregation prone model polypeptide, we show that autophagy deficient cells accumulate insoluble Ex1HttQ97-EGFP more rapidly and form greater numbers of IBs compared to autophagy proficient cells. Re-expression of Atg5 in Atg5 deficient cells reversed this phenotype. Most strikingly, rapamycin reduced the amount of insoluble Ex1HttQ97-EGFP and IBs to a similar degree in both Atg5^{+/+} and Atg5^{-/-} cells. The formation of SDS-insoluble polyQ assemblies is a cooperative process that is highly dependent on the accumulation of a critical mass of the protein (Scherzinger et al., 1999; Colby et al., 2006). We suggest that a major effect of rapamycin is the reduction in protein synthesis required for polyQ aggregation and IB formation to occur.

Materials and Methods

Expression vectors. Mammalian expression vectors encoding exon 1 of the HD gene with 25 or 97 glutamines fused at the C-terminus to a EGFP tag were a gift from Erich Schweitzer and Alan Tobin (Brain Research Institute, University of California, Los Angeles, CA 90095, USA). The mouse Atg5 expression vector and adenovirus mRFP-LC3 have been described previously (Mizushima et al., 2001; Bampton et al., 2005).

Cell culture, transfection, inclusion load measurement and microscopy. SV-40 transformed MEF from Atg5^{+/+} and Atg5^{-/-} mice (Kuma et al., 2004) were cultured in Dulbecco's Modified Eagle's Medium (DMEM; Gibco) containing 10% foetal bovine serum (FBS; Sigma), 4.5 g/L Glucose, 2 mM L-glutamine, 1 mM sodium pyruvate, 100 U/ml penicillin and 100 µg/ml streptomycin (Sigma) in 5% CO₂ at 37°C. Cells were propagated in 75 cm² flasks and seeded on 12 mm poly-L-lysine coated glass cover slips in 24-well plates for fluorescence analysis or directly onto 6-well plates for immunoblot/filter-trap analysis. Cells were trypsinised, counted and seeded at a density of 4 x 10⁴ cells per well in 24-well plates and 3 x 10⁵ cells per well in 6-well plates. After an overnight culture, cells reached 60-80% confluence and were transiently transfected using Lipofectamine 2000 reagent (Invitrogen) according to the manufacturer's instructions. The transfection medium was replaced with fresh medium after 4 h and cultures were incubated for a further 20 h in the presence or absence of the following inhibitors: 200 nM rapamycin (Rap; Sigma), 50 nM bafilomycin A1 (BafA1; Sigma), 0.3 to 0.01 µg/ml cycloheximide (CHX; Sigma). Cultures requiring longer time-courses were split 24 hours after transfection and re-seeded at lower densities for harvesting after 48 to 96 hours. Cells were fixed in 4% paraformaldehyde, washed in PBS, and analysed using epifluorescence microscopy with an Olympus X-170 microscope. Images were collected using an AstraCam camera and UltraView™ software (PerkinElmer). Inclusion load was calculated as the proportion of EGFP-expressing cells that contained inclusion bodies (IBs). At least 200 cells were counted per condition.

Protein synthesis and cell counting. Cells were briefly washed free of methionine to avoid long-term methionine deprivation and labelled for 1 h in methionine-free RPMI medium (Sigma) containing 10% FBS and 1.85 MBq [³⁵S]methionine (SJ1515, Amersham) and the appropriate additives. Cells were washed 3 times in methionine-containing DMEM, protein was precipitated in ice-cold 20%

trichloroacetic acid, and after 3 washes with 5% trichloroacetic acid, the precipitate was dissolved in 15% SDS and radioactivity was measured by scintillation counting. Little tRNA was found in these pellets. Cells were counted after trypsinisation using a haemocytometer.

Immunoblotting, immunocytochemistry, filter trap assay, and re-solubilisation with formic acid.

Cells were either collected with a cell scraper, or trypsinised and counted using a haemocytometer before being pelleted and washed in phosphate buffered saline (PBS). Material was prepared for immunoblotting and filter-trap detection according to Wanker et al. (1999). Briefly, cells were lysed on ice for 30 minutes in filter-trap lysis buffer (50 mM Tris-HCl, pH 8.8, 100 mM NaCl, 5 mM MgCl₂ 0.5% (w/v) NP-40, 1 mM EDTA) in the presence of Complete™ protease inhibitors (Roche). Insoluble material was pelleted by centrifugation at 16,000 x g for 10 min and resuspended in 100 µl DNaseI buffer (20 mM Tris-HCl, 15 mM MgCl₂, 0.5 mg/ml DNase I (Sigma)) for 2 h at 37°C. Protein concentrations of soluble (supernatant fraction) and insoluble fractions (pellet) were determined using the Bicinchoninic acid kit (Sigma) and BSA standards. Between 5 and 30 µg of insoluble material was diluted into 200 µl 2% SDS, boiled for 5 min, and applied to a 96-well dot blot apparatus (BioRad) containing a cellulose acetate membrane with 0.2 µm pore-size (Macherey-Nagel). Resolubilisation of pellets with formic acid was performed according to Hazeki et al. (2000). Pellets were treated in 100 µl 100% formic acid for 1 hour at 37°C, vacuum centrifuged and solubilised in 1x SDS PAGE sample buffer (see below). Soluble material was supplemented with 4x SDS-PAGE sample buffer (1 M Tris-HCl pH 6.8, 400 mM DTT, 8% SDS, 40% glycerol) and 30 µg was used for analysis by SDS-PAGE (8% to 12.5%). Membranes were blocked in 5% milk for 1 hour and probed with the following primary antibodies: mouse monoclonal anti-GFP (8371-1, BD Biosciences at 1:4000, rabbit polyclonal anti-phospho-S6 (2211, Cell Signalling) at 1:1000, mouse monoclonal anti-ERK (M12320, Transduction laboratories) at 1:5000, rabbit polyclonal anti-actin (A2066, Sigma) at 1:1000, mouse anti-vimentin (V6630, Sigma, 1:40). ICC was performed as in Bampton et al. (2005). Rabbit polyclonal anti-LC3 antibodies were gifts from Yasuo Uchiyama (Osaka University Graduate School of Medicine, Osaka 565-0871, Japan and Eiki Kominami (Juntendo University School of Medicine, Tokyo, 113-8421 Japan). Rabbit polyclonal anti-Atg5 antibody was described previously (Mizushima et al., 2001). Blots were subsequently probed with HRP-conjugated anti-mouse or anti-rabbit IgG (Jackson ImmunoResearch Laboratories) at 1:5000 and visualised with ECL detection reagents (Amersham). Immunoblots and dot blot signals were scanned with a flat bed scanner (hp scanjet 5470c, Hewlett

Packard) and densitometry was performed using ImageJ software (NIH). For ratiometric values, the integrated pixel intensity of each signal was calculated and divided by the signal intensity obtained under control conditions. For each sample, dot plots were repeated at 2-3 dilutions to ensure that the signal was not saturated, giving rise to a single value used for statistical analysis. Values from several experiments were then used to determine the mean (fold) difference in signal intensity. Input was normalised either according to cell number or protein content. For SDS-insoluble material, in some experiments a parallel analysis of protein loading was conducted by immunoblotting for histone expression (MAK, PhD Thesis, data not shown).

Statistical analysis. The mean value of replicates within an experiment (duplicates to quadruplicates) was taken as a single value when calculating standard deviations from multiple experiments. Multiple comparisons were made using ANOVA followed by Tukey's HSD posthoc test, pair-wise comparisons were conducted using two tailed Student's t-test, and one sample t-test or 95% confidence intervals were used for calculating the significance of ratiometric values. These values and the number of experiments performed for each result are indicated in the text and figure legends.

RESULTS

Genetic ablation of Atg5 increases Ex1HttQ97-EGFP accumulation and inclusion body formation.

We first tested whether the complete genetic ablation of autophagy (Atg5) in cells (mouse embryonic fibroblasts, MEF) modulated the accumulation of polyQ-expanded huntingtin (htt) as previous experiments have been performed with RNAi approaches or not under conditions of htt synthesis (Iwata et al., 2005b; Shibata et al., 2006). Atg5^{+/+} and Atg5^{-/-} MEFs were transfected with cDNA encoding exon 1 of human htt containing either 25 glutamines (Ex1HttQ25) or 97 glutamines (Ex1HttQ97) fused to enhanced green fluorescent protein (EGFP). No discernable inclusion bodies (IBs) in cells were found in MEFs of either type transfected with Ex1HttQ25-EGFP (Fig. 1). However, cytoplasmic or nuclear IBs were readily formed in Ex1HttQ97-EGFP-expressing cells of both types (Fig. 1). Evidence that Atg5^{+/+} MEFs were proficient to undergo autophagy whilst Atg5^{-/-} MEFs were not was obtained by expression of mRFP-LC3. Fig. 1 shows that Atg5^{+/+} MEFs contained several mRFP-LC3 puncta while mRFP-LC3 expression in Atg5^{-/-} MEFs was evenly diffuse, as shown previously (Bampton et al., 2005). We did not observe co-localisation of mRFP-LC3 with IBs in wt cells at this time point (24 h).

The proportion of EGFP-expressing cells containing IBs increased over time in both cell types (Fig. 2A). About twice as many Ex1HttQ97-EGFP-positive Atg5^{-/-} MEFs contained IBs compared to Atg5^{+/+} MEFs after 1-2 days (Fig. 2A). Nuclear inclusions in ca. 10-15% of both types of cells were evident from the fact that nuclear DNA was “vacated” from spots where the IBs had deposited (Fig. 1, arrows) (for quantification see Fig. 4). There was no difference in the transfection rate between Atg5^{-/-} and Atg5^{+/+} cells (quantified in Fig. 4), transfection efficiency varying between 50-60% in both types of MEFs (see Supplementary Fig. S1 for low power fluorescent images of cells). It is important to note that at 24 h after transfection, we did not detect any differences in toxicity caused by either Ex1HttQ25-EGFP or Ex1HttQ97-EGFP expression in Atg5^{+/+} and Atg5^{-/-} cells as assessed by inspection of nuclear abnormalities (ca. 5% of EGFP +ve cells showed baseline toxicity as measured by nuclear fragmentation; see Fig. 4 for a quantitative comparison). Therefore the increase in IB formation of Ex1HttQ97-EGFP in Atg5^{-/-} cells was neither due to unequal transfection nor to any differential toxicity due to IB formation in our experiments.

To test whether the increase in IBs in the Atg5^{-/-} cells relative to Atg^{+/+} cells correlated with an increase in the accumulation of SDS-insoluble Ex1HttQ97-EGFP, we used the filter trap assay to measure the amount of SDS-insoluble Ex1Htt-Q97 protein formed in each cell type. Pellets remaining

after protein extraction in 1% NP-40 were treated with DNase I, boiled in 2% SDS, and filtered onto a cellulose acetate filter using a dot blot apparatus (Wanker et al., 1999) while respective supernatant proteins were separated by SDS-PAGE. Fig. 2B shows that Ex1Htt-Q97 formed SDS-insoluble material in both types of MEFs while Ex1Htt-Q25 did not. Quantification showed that there was a two-fold increase of insoluble Ex1HttQ97-EGFP in Atg5^{-/-} cells compared to Atg5^{+/+} cells hence correlating with increased IB formation in autophagy-deficient versus autophagy-proficient cells (Fig. 2D, filled bars, n=4, p<0.001).

To test for autophagic activity, we probed for LC3 by immunoblotting. Consistent with the lack of mRFP-LC3 puncta in Atg5^{-/-} MEFs (Fig. 1B), no LC3 II was detected in Atg5^{-/-} extracts from Atg5^{-/-} cells immunoblotted for LC3 but extracts from Atg5^{+/+} MEFs expressed LC3 II, the latter being the autophagosome-associated form of LC3. A similar amount of LC3 I was expressed in both cell types. Equal input of soluble protein was confirmed with an antibody against ERK1 and 2 (tERKs). Further evidence for ongoing autophagy in Atg5^{+/+} cells was obtained by treatment with bafilomycin A1 (BafA1), which prevents LC3 II degradation in lysosomes and thus causes LC3 II to accumulate in autophagically-proficient cells (Kabeya et al., 2001; Bampton et al., 2005). Figure 2C shows that BafA1 significantly increased the amount of LC3 II in Atg5^{+/+} cells compared to untreated cells while no changes in LC3 occurred in Atg5^{-/-} cells, consistent with the complete absence of autophagy in these cells. Blocking autophagy using BafA1 also significantly increased SDS-insoluble Ex1httQ97-EGFP in the autophagy-proficient but not autophagy-deficient cells (Fig. 2C, quantified in Fig. 2D). The ratio of LC3 II/I varied between experiments (Fig. 2B and C), but BafA1 always increased the amount of LC3 II by at least 2-fold (Fig. 2D). No SDS-insoluble material was detected in extracts of Ex1htt-Q25-EGFP transfected cells of either genotype (Fig. 2B). We also did not detect EGFP signals on filters when filtrating the supernatant of Ex1HttQ97-EGFP-expressing cells after spinning at 16,000 x g (data not shown) but without boiling, suggesting that no SDS-insoluble oligomeric Ex1HttQ97-EGFP species of more than 200 nm (pore size of filter) were generated.

We analysed whether the IBs are ubiquitinated in both cell types as this is a hallmark of all polyQ diseases *in vivo* including HD. We found co-localisation of ubiquitin with IBs in ~5% of both Atg5^{+/+} and Atg5^{-/-} cells (Fig. 3 and data not shown). We also found that LAMP-1 (lysosome-associated membrane protein) was associated with IBs in both cell types. Because cytoplasmic IBs are surrounded by intermediate filaments that form an “aggresome” (Waelter et al., 2001), we further probed for the intermediate filament protein vimentin. In both Atg5^{-/-} and Atg5^{+/+} cells IBs were

surrounded by vimentin immunoreactivity. These results show that IBs are qualitatively similar in both cell types.

Together these data show that Atg5-dependent degradation via autophagy plays an important role in determining the amount of insoluble polyQ-expanded Ex1Htt protein. The decrease in the propensity of cells to form IBs and insoluble Ex1HttQ97-EGFP correlates with their ability to perform autophagy.

Rapamycin reduces the amount of insoluble Ex1HttQ97-EGFP and inclusion body formation in both autophagy-proficient and -deficient cells

We next investigated whether rapamycin requires an Atg5-dependent mechanism to modulate the amount of insoluble Ex1HttQ97-EGFP and IB formation. MEFs were treated with 200 nM rapamycin either 12 h before transfection, to instil high autophagic activity prior to onset of polyQ expression and IB formation, or treated with rapamycin simultaneously with transfection. After 18-24 h, the percentage of EGFP-positive cells with IBs was determined while insoluble Ex1HttQ97-EGFP was measured using the filter trap assay as described above. To determine that rapamycin was active, we measured S6 phosphorylation. S6 is a ribosomal protein whose phosphorylation is regulated by S6 kinase in an mTOR-dependent manner (Nobukini and Thomas, 2004). Fig. 4A shows that rapamycin added 12 h prior to transfection inhibited S6 phosphorylation in both cell types (transfected with Ex1HttQ25-EGFP or Ex1HttQ97-EGFP), indicating that rapamycin prevented mTOR activity independently of Atg5 activity. There was no difference in the amount of Ex1HttQ25-EGFP or Ex1HttQ97-EGFP expressed in either cell type treated with rapamycin compared to untreated cells when the total amount of soluble protein input was equalised between treatments, thus indicating that there is no differential destruction of the transfected proteins per se (Fig. 4A).

Pre-treatment with rapamycin significantly decreased the proportion of EGFP-positive cells containing Ex1HttQ97-EGFP IBs by 40-45% in both Atg5^{+/+} and Atg5^{-/-} MEFs (Fig. 4B). To ensure that rapamycin treatment did not affect the transfection efficiency or toxicity of the Ex1Htt transgenes in either Atg5 cell type we monitored both. We and others have previously shown that analysis of nuclear morphology as measured by nuclear fragmentation and condensation using DNA stains is a reliable marker of cell toxicity under these conditions and strongly correlates with other markers of cell death (Wytenbach et al., 2001). Figure 4C shows that the toxicity associated with expression of Ex1HttQ25- or Q97-EGFP was at a baseline level (5%) under our experimental conditions (after 18-24 hours after

transfection) and not different in the two Atg5 cell types (white bars). Furthermore, rapamycin treatment did not modulate cell survival compared to control conditions (black bars), demonstrating that the reduction of IBs in the both Atg5 cell lines induced by rapamycin (Fig. 4B) was not due to a differential toxicity (mean \pm SD, n=3, ANOVA p=0.6). To make sure that the differential increase in IBs between Atg5^{+/+} and Atg5^{-/-} cells (Fig. 2B and Fig. 4B) and the decrease in IB formation by rapamycin was not due to unequal transfection rates, we measured the transfection under the various conditions by counting the number of EGFP positive cells in the total cell population after each experiment in parallel with the analysis of toxicity and IB. As shown in Figure 4D we obtained transfection efficiencies of 50-60%. Importantly, neither the cell type nor rapamycin affected the rate of transfection (mean \pm SD, n=3, ANOVA p=0.3). As we observed a minor proportion of IBs in the nuclear compartment (Fig. 1) we also quantified the proportion of Atg5^{+/+} and Atg5^{-/-} cells containing IB located in the nucleus versus cytoplasmic localisation and whether this distribution is modulated by rapamycin. Figure 4D shows that the 10-15% of nuclear IBs in both cell types was not changed under rapamycin treatment (mean \pm SD, n=3, ANOVA p=0.9).

Having shown that rapamycin treatment reduced IBs in both cell types we next investigated whether this reduction was also observed in the amount of insoluble material. IBs are cellular structures (or aggresomes) that may not provide an adequate estimation of the amount of polyQ aggregation. However, we measured a similar reduction in SDS-insoluble Ex1HttQ97-EGFP induced by rapamycin when this was assayed by filter trap, or after solubilising the SDS-insoluble pellet with formic acid, thereby controlling for equal protein input and loading between the different conditions (Fig. 5A, quantified in B). There was no significant change in the amount of insoluble Ex1HttQ97-EGFP formed in cells that had been treated with rapamycin at the time of transfection compared to control (see supplementary Fig. S2 for raw data). Thus, rapamycin can decrease the amount of insoluble Ex1HttQ97-EGFP and IB load, but this effect occurs in an Atg5-independent manner, and with a considerable delay following its addition.

Ravikumar et al (2004) found that mTOR was inactivated in polyQ-expressing cells, was bound to a polyQ expanded N-terminal portion of Htt and sequestered into IBs and thus suggested that autophagy is endemically activated in HD (and maybe other polyQ diseases) as a protective response. In MEFs expressing Ex1HttQ97-EGFP, we failed to find an increase in mTOR immunoreactivity after solubilisation of IBs using formic acid. mTOR was also not trapped on the stacking gel in conjunction

with Ex1HttQ97-EGFP (data not shown) so the degree of sequestration of mTOR may be cell-specific and time dependent.

Our finding that rapamycin reduced IBs and SDS-insoluble material in autophagy-deficient cells was unexpected. Hence we next investigated through which mechanism rapamycin reduced IBs and SDS-insoluble Ex1htt-Q97-EGFP.

Rapamycin reduces formation of insoluble Ex1HttQ97-EGFP by lowering the amount of soluble protein input

To investigate how rapamycin may be reducing the load of insoluble Ex1HttQ97-EGFP and IBs in Atg5^{-/-} MEFs, the kinetics of cell cycle and protein expression were investigated, since rapamycin is well documented to be a cell cycle suppressant and an inhibitor of protein synthesis (Dann and Thomas, 2006; Sabbatini, 2006). To measure this we counted the number of cells and calculated the amount of decrease due to rapamycin treatment compared to untreated cells set as the control value (presented as % change). Indeed, ca. 25% fewer cells were generated in rapamycin-treated MEFs over the experimental period (36 h) irrespective of Atg5 genetic background or expression of Ex1HttQ25-EGFP or Ex1HttQ97-EGFP (Fig. 6A, first panel. 0.001<p<0.05 for every condition relative to untreated control; see supplementary Fig. S3 for raw data). There was no statistical difference in rapamycin-induced decrease in cell number between untransfected cells or cells transfected with Ex1httQ25-EGFP or Ex1HttQ25-EGFP. The reduction in total cell protein in rapamycin-treated cultures compared to untreated cultures was about 37% irrespective of Atg5 genetic status or Ex1HttQ25-EGFP or Ex1HttQ97-EGFP expression (Fig. 6A, second panel; 0.001<p<0.05 for every condition relative to untreated control; see supplementary Fig. S3 for raw data) and no difference in the amount of this reduction between untransfected or transfected cells with either construct under rapamycin treatment was observed. When the total amount of protein per cell was calculated, the amount of protein was diminished on average by $17 \pm 1.8\%$ in rapamycin-treated cells compared to that in untreated controls irrespective of genetic background or expression of Ex1HttQ25-EGFP or Ex1HttQ97-EGFP proteins (Fig. 6A, third panel). Thus, we conclude that rapamycin caused a significant reduction in protein per cell (p<0.001, t-test on pooled results, n=10 for each genotype).

To test whether the reduction in total protein/cell due to rapamycin treatment included protein translated from Ex1htt expressing plasmid, we examined the amount of Ex1HttQ25-EGFP produced to avoid the uncertainty associated with the insolubility of Ex1HttQ97-EGFP (Ex1httQ25-EGFP is soluble

under all conditions examined, see above). Fig. 6B shows that the average reduction in expression of Ex1HttQ25-EGFP per cell due to rapamycin was about 14% in both Atg5^{+/+} and Atg5^{-/-} cells, similar to the reduction found in total protein per cell. There was no statistical difference in the reduction of total protein per cell and the reduction of Ex1HttQ25-EGFP per cell due to rapamycin treatment. This finding also suggests that Atg5 null cells have no increased protein expression from the plasmids compared to Atg5 wildtype cells due to the lack of the autophagic protein degradation system.

We next measured whether the reduction of 37% of total protein per cell due to rapamycin treatment (Fig. 6A) was correlating with a similar reduction in global protein synthesis as measured by direct [³⁵S]methionine incorporation. Thirty hours after addition of rapamycin we added [³⁵S]methionine to Atg5^{+/+} cells for 1 h. We observed a significant reduction in [³⁵S]methionine incorporation (Fig. 6C; mean ± SD, n=3; t-test p<0.001). We then quantified the reduction as a percentage change under rapamycin treatment compared to untreated cells and found that there was a 39 ± 3% reduction in [³⁵S] Met incorporation (Fig. 6D, first bar). This 39% reduction was almost identical to the reduction of 37 ± 3% found for total soluble protein (Fig. 6d, second bar) that we calculated in parallel in each of these experiments. Calculating the ratio of change in [³⁵S]methionine incorporation over the reduction of total protein content, this value was no different from zero indicating that the reduction in the global amount of protein (as shown in Fig. 6A and D) is likely to be due to an inhibition of protein synthesis.

Inhibition of protein synthesis by cycloheximide reduces the level of insoluble Ex1HttQ97 and inclusion body formation similar to rapamycin

To investigate how a decrease in protein synthesis per cell affects the propensity of cells to form insoluble Ex1HttQ97-EGFP and IBs, a concentration of cycloheximide (CHX), an inhibitor of protein synthesis, was sought that matches the decrease in the amount of soluble protein obtained with rapamycin. Cycloheximide was used because it binds to ribosomes reversibly thus ensuring a response that is proportional to ribosome occupancy over extended periods of treatment. In dose-response experiments using rapamycin, we did not observe a significant difference in the amount of reduction in global protein synthesis between 50-200 nM rapamycin (data not shown) and hence we aimed at a CHX concentration that would match that induced by 200 nM rapamycin.

As expected, the amounts of insoluble Ex1HttQ97-EGFP protein (Fig. 7A) and IB formation (Fig. 7B) were highly dependent on the concentration of CHX used in both cell types. Between 0.03-0.1 µg/ml CHX, a similar amount of insoluble Ex1HttQ97-EGFP was detected in the filter trap assay

compared to the insoluble material obtained from rapamycin treated cells (200 nM) irrespective of Atg5 genetic status (Fig. 7A). The amount of IBs formed with rapamycin also closely matched that observed with this concentration range of CHX (Fig. 7B), the amount of insoluble Ex1HttQ97-EGFP and IB formation being equally reduced. Moreover, steady state protein levels were reduced similarly by the same range of CHX and rapamycin (see Supplementary Fig. 5S). Finally, when we compared the amount of [³⁵S]methionine incorporation over 1 h in cells pre-treated with rapamycin (200 nM) and cells pre-incubated with different concentrations of CHX for 24 h, a similar inhibition of [³⁵S]methionine incorporation was found with rapamycin and ca. 0.02 µg/ml CHX (rapamycin: 41.1 ± 7.2% compared to 49 ± 4% with 0.02 µg/ml CHX, mean ± range, 2 independent experiments). This result suggests that a concentration of CHX that similarly inhibits protein synthesis compared to 200 nM rapamycin also produces equivalent reduction in insoluble Ex1HttQ97-EGFP and IBs obtained by 200 nM rapamycin. Hence, a small reduction in the input of Ex1HttQ97-EGFP has major effects on the kinetics of formation of insoluble Ex1HttQ97-EGFP and IBs. Interestingly, at higher concentrations (0.1-0.3 µg/ml) CHX also reduced the amounts of LC3 I/II in Atg^{+/+} and LC3 I in Atg^{-/-} cells to an equivalent extent by the end of the treatment (Fig. 7A), suggesting that LC3 protein is being turned over quite quickly during this time by non-autophagic mechanisms.

Atg5 overexpression partially restores autophagic activity in Atg5^{-/-} cells and reduces insoluble polyQ expanded Ex1Htt.

The characteristics of cell lines can diverge rapidly even when they derive from a common origin. To further investigate the role of autophagy in the control of insoluble Ex1HttQ97-EGFP and IB load, Atg5 was expressed in Atg5^{-/-} and Atg5^{+/+} cells by transfection. Atg5 expression in Atg5^{-/-} cells induced the formation of the Atg5/Atg12 conjugate and restored the ability of the cells to produce LC3 II to about 20% of the levels measured in Atg5^{+/+} cells (Fig. 8A). Interestingly, we found co-localisation of overexpressed Atg5 with IBs (see Supplementary Fig. 4SA) and a significant amount of Atg5 (but not Atg5/12 conjugate) accumulated in the pellets of both types of MEF cells expressing Ex1HttQ97-EGFP (Supplementary Fig. 4SB shows results for Atg5^{-/-} cells). Whether this Atg5 is disabled from performing its function (as no Atg12 accumulated in this fraction) remains to be resolved. Together these results suggest that some of the overexpressed Atg5 protein in Atg5^{-/-} cells is functional, consistent with the recent finding of Hosokawa et al., (Hosokawa et al., 2006) using the same cell clone and DNA plasmids.

When the amount of insoluble material was examined using the filter trap assay (Fig. 8B), overexpression of Atg5 in Atg5^{-/-} cells reduced the amount of insoluble material that accumulated each day. Already after 1 day, the amount of insoluble Ex1HttQ97-EGFP in Atg5^{-/-} cells expressing Atg5 decreased by $27 \pm 8\%$ compared to $2 \pm 1\%$ change in Atg5^{+/+} cells (mean \pm SEM, n=4, p<0.02, t test; Fig. 8C). To compare the rate of reduction of insoluble Ex1Htt-Q97-EGFP under conditions of Atg5 overexpression over several days, we split and replated the transfected cells after 2 days of transfection and measured the rate of decrease of Ex1Htt-Q97-EGFP in both cell types (Fig. 8D). Atg5 overexpression accelerated the reduction of Ex1Htt-Q97-EGFP in Atg5^{-/-} cells, but not in Atg5^{+/+} cells. It is important to note that overexpression of Atg5 did not reduce the amount of total protein harvested from the Atg5^{-/-} or Atg5^{+/+} cells (unlike rapamycin), suggesting that the decrease in Ex1HttQ97-EGFP caused by Atg5 is independent of protein synthesis (data not shown). Moreover, the number of cells harvested at each time point was similar between the four conditions, demonstrating that Atg5 overexpression had no effect on the cell cycle. It should be noted that insoluble Ex1Htt-Q97-EGFP also decreases over time in cells not overexpressing Atg5 from day 2-4 (Fig. 8B, D). This is likely due to continuous cell division, which reduces the number of plasmids present in each cell. A differential loss of cells containing insoluble Ex1Htt-Q97-EGFP between day 2-4 may also contribute to this finding. Together, these data show that re-expression of Atg5 in autophagy-deficient cells achieves a reduction in the amount of insoluble Ex1HttQ97-EGFP.

Discussion

In the present paper we show that autophagy-deficient cells lacking Atg5 expression accumulate more misfolded insoluble polyQ protein (Ex1HttQ97-EGFP) and form more inclusion bodies (IBs) than control cells and that this effect can be partially reversed by re-expressing Atg5. These data suggest that the lack of autophagy increases polyQ aggregation and/or reduces clearance of aggregation-prone polyQ proteins. Our results obtained through a genetic approach (complete genetic knockout of Atg5) are consistent with those of recent studies (Kouroku et al., 2006, Iwata et al., 2005a,b)

Rapamycin is a well-characterised activator of autophagy and has previously been reported to alleviate toxicity of different aggregate-prone proteins (Rubinsztein, 2006). In these reports the authors suggested that the beneficial effects of rapamycin resulted from its ability to reduce aggregation-prone toxic proteins via autophagy. Hence one would predict that rapamycin would reduce polyQ aggregation in autophagy-proficient cells, but not in autophagy-deficient cells. We tested this idea by treating Atg5^{+/+} and Atg5^{-/-} cells with rapamycin and found that rapamycin reduced soluble and insoluble aggregate-prone Ex1Htt fragments independent of autophagic activity. The evidence for this effect of rapamycin is as follows: a) rapamycin reduced insoluble Ex1HttQ97 and IB load in Atg5 null cells. b) inhibition by rapamycin, which rapidly inhibited phosphorylation of S6 kinase within 1 h, was only apparent if the cells were preincubated with rapamycin for about 12 h prior to expression of Ex1HttQ97 for 24 h, a time frame that suggests long-term rather than short term actions of the drug are required for the effect to occur. c) rapamycin reduced the amount of soluble protein per cell within this time frame by about 17% in both Atg5^{+/+} and Atg5^{-/-} cells, and this amount of inhibition was correlated with the amount of [³⁵S]methionine incorporated over 1 h at the end of the incubation period, indicating that the reduction in global protein/cell occurred because of a reduction in protein synthesis. The similar extent of rapamycin-induced reduction in the amount of soluble Ex1HttQ25-EGFP per cell indicates that protein synthesis from the plasmid was similarly affected. d) the reduction in SDS-insoluble polyQ aggregation and IB formation induced by rapamycin could be mimicked by use of low concentrations of CHX, which also caused a similar partial reduction in the extent of [³⁵S]methionine incorporation. Thus, it appears that treatment with rapamycin can critically impact on the mass of soluble protein required for polyQ aggregation and IB formation independently of autophagy through a relatively modest reduction in protein input.

It is likely that autophagy too can reduce polyQ aggregation not only through clearance of formed polyQ aggregates, but also by reducing the amount of polyQ protein submitted to these processes. These two mechanisms could be acting in an additive way. It is conceivable that some of the effects of rapamycin observed in previous studies may be due to a reduction in protein synthesis. In two studies where rapamycin was used during the period of Htt synthesis (*Drosophila*, transgenic mice) (Berger et al., 2006), it was not reported whether there were changes in expression levels of the transgenes and hence it is possible that some of the protective effects were due to the inhibitory action of rapamycin on translation. However, a subtle reduction in the synthesis of an Htt fragment due to rapamycin may be difficult to detect in animal models. Rapamycin treatment has been proposed to inhibit translation of specific mRNAs rather than resulting in global inhibition of translation (Grolleau et al., 2002). However, we found similar amounts of reduction in total protein per cell and in the amount of Ex1HttQ25-EGFP synthesised per cell, suggesting that there is no selectivity in nuclear versus plasmid-based CMV promoter mediated expression. At present, we cannot distinguish between a possible effect of rapamycin on global translation versus a more specific effect on a subset of mRNAs although it is clear that the function of some genes required for cell cycle are suppressed.

An interesting question is whether rapamycin mediates all its effects through mTOR. To date there are no known alternative targets of rapamycin other than FK506 binding protein 12, which inhibits the protein kinase mTOR (Wullschleger et al., 2006), suggesting that the inhibitory effects of rapamycin on the synthesis (this study) and the clearance of aggregate prone proteins via autophagy (see Rubinstein, 2006) occur via mTOR. However, not all the effects of mTOR are mediated by autophagy. The serine/threonine kinase mTOR is a highly conserved integrator of mitogenic and nutrient inputs and controls cell proliferation, cell growth and endocytosis. These activities are likely mediated through modulation of protein synthesis (Dann and Thomas, 2006; Wullschleger et al., 2006), consistent with our observation of a reduction in insoluble Ex1HttQ97-EGFP and IBs in the autophagy-deficient Atg5^{-/-}MEFs. The extent of inhibition of protein synthesis of about 17% we observe is in keeping with the reported decrease of 15-50% in translation rates induced by mTOR inhibition in mammalian cells (whereas in yeast, inhibition is nearer 100%) (Jefferies et al., 1994; Terada et al., 1994). Hence, it is likely that the effect of rapamycin on protein synthesis is cell type dependent. It remains to be seen to what extent this drug affects protein synthesis in neurons.

The reduction in insoluble Ex1HttQ97-EGFP achieved with rapamycin was mimicked by use of CHX. Several reports have demonstrated that CHX inhibits autophagy (Kovacs and Seglen, 1981) by

preventing fusion of autophagosome with endo/lysosomes (Lawrence and Brown, 1993). Consistent with this view, IBs were cleared more quickly in the presence of rapamycin in an inducible cell model after expanded httEx1 protein synthesis was turned off but IBs appeared to accumulate when CHX (10 $\mu\text{g/ml}$) was present with rapamycin (Ravikumar et al., 2002). In the above papers 2-10 $\mu\text{g/ml}$ CHX was used, which inhibits protein synthesis and autophagy over 95% whereas in our study, the concentration that mimicked rapamycin's effect was between 0.01-0.03 $\mu\text{g/ml}$, which elicited only a partial block on protein synthesis and presumably on autophagy. However, our important observation is that the same reduction in insoluble material and IBs were elicited by CHX in Atg5^{-/-} MEFs, where no autophagy can take place. Hence the phenomenon we observed here is unlikely to be related to autophagy.

Autophagic clearance of Htt fragments may be promoted independently of mTOR (and S6K/Akt) via a pathway dependent on insulin receptor substrate 2 (IRS2) and stimulated via insulin and IGF-1 (Yamamoto et al., 2006). The notion that there are mTOR-independent pathways of autophagy is suggested by the finding that rapamycin inhibited autophagy suppression by insulin but not by regulatory amino acids in liver cells (Kanazawa et al., 2004) and yeast susceptibility to osmotic stress differed when induction of autophagy was by starvation or rapamycin (Prick et al., 2006). Indeed, it has recently been shown that small-molecule enhancers of mammalian target of rapamycin (mTOR) can act independently of rapamycin to enhance clearance of mutant huntingtin fragments and A53T alpha-synuclein (Sarkar et al., 2007). These findings suggest that multiple mechanisms may regulate autophagic clearance of misfolded/aggregated proteins. However, irrespective of how the proteins are cleared, a reduction in the critical mass of aggregation-prone proteins such as that described in the present study will always be beneficial in reducing protein aggregation.

Reducing the expression of Htt is in theory a promising strategy to alleviate disease: a decrease in expression of wildtype Htt up to 50% is not detrimental (based on studies in heterozygotes) while decreasing the expression of mutant Htt using an siRNA approach has been found to significantly reduce HD pathology in mice (Wang et al., 2005; Machida et al., 2006). This idea is supported by the recent findings of Colby et al (Colby et al., 2006) who proposed that an efficient therapeutic strategy for HD lies in reducing the rate of mutant Ex1Htt aggregation by only modestly reducing Htt expression levels. From our study we cannot conclude however that rapamycin would have a beneficial effect by reducing htt synthesis in all cases. Future *in vivo* studies will be required to address this point.

It is important to note that in HD *in vivo*, mutant Htt is constantly produced, hence the mechanisms by which rapamycin regulates the accumulation and turn-over of mutant Htt should be

studied under condition of continuous Htt expression as we have done in our cellular model. The stochastic model of Colby et al. (2006) was applied under conditions where no further protein synthesis was taking place during the misfolding process. If rapamycin can reduce Htt concentrations in HD, it might be beneficial even under conditions where autophagy is already working at its maximal rate.

Acknowledgements

We thank Dr Yasuo Uchiyama (Osaka University Graduate School of Medicine, Osaka 565-0871, Japan and Dr Eiki Kominami (Juntendo University School of Medicine, Tokyo, 113-8421 Japan) for provision of anti-LC3 antibodies, and Drs Eric Schweitzer and Alan Tobin for the original constructs of Ex1htt-Q25-EGFP and Ex1htt-Q97-EGFP. Most of this work was conducted in AMT's lab under joint supervision of AW and AMT.

References

Bampton ETW, Goemans CG, Niranjana D, Mizushima N and Tolkovsky AM (2005) The dynamics of autophagy visualised in live cells: from autophagosome formation to fusion with endo/lysosomes. *Autophagy* **1**: 23-36.

Berger Z, Ravikumar B, Menzies FM, Oroz LG, Underwood BR, Pangalos MN, Schmitt I, Wullner U, Evert BO, O'Kane CJ and Rubinsztein DC (2006) Rapamycin alleviates toxicity of different aggregate-prone proteins. *Hum Mol Genet.* **15**: 433-442.

Colby DW, Cassady JP, Lin GC, Ingram VM and Wittrup KD (2006) Stochastic kinetics of intracellular huntingtin aggregate formation. *Nat Chem Biol* **2**: 319-323.

Cummings CJ and Zoghbi HY (2000) Trinucleotide repeats: mechanisms and pathophysiology. *Annu Rev Genomics Hum Genet.* **1**: 281-328.

Dann SG and Thomas G (2006) The amino acid sensitive TOR pathway from yeast to mammals. *FEBS Lett* **580**: 2821-2829.

Grolleau A, Bowman J, Pradet-Balade B, Puravs E, Hanash S, Garcia-Sanz JA and Beretta L (2002) Global and specific translational control by rapamycin in T cells uncovered by microarrays and proteomics. *J Biol Chem.* **277**: 22175-22184.

Hazeki N, Takamoto T, Goto J and Kanazawa I (2000) Formic acid dissolves aggregates of an N-terminal huntingtin fragment containing an expanded polyglutamine tract: applying to quantification of protein components of the aggregates. *Biochem Biophys Res Commun* **277**: 386-393.

Hosokawa N, Hara Y and Mizushima N (2006) Generation of cell lines with tetracycline-regulated autophagy and a role for autophagy in controlling cell size. *FEBS Lett.* **580**: 2623-2629.

Iwata A, Christianson JC, Bucci M, Ellerby LM, Nukina N, Forno LS and Kopito RR (2005a) Increased susceptibility of cytoplasmic over nuclear polyglutamine aggregates to autophagic degradation. *Proc Natl Acad Sci U S A*. **102**: 13135-13140.

Iwata A, Riley BE, Johnston JA and Kopito RR (2005b) HDAC6 and microtubules are required for autophagic degradation of aggregated huntingtin. *J Biol Chem*. **280**: 40282-40292.

Jana NR and Nukina N (2003) Recent advances in understanding the pathogenesis of polyglutamine diseases: involvement of molecular chaperones and ubiquitin-proteasome pathway. *J Chem Neuroanat*. **26**: 95-101.

Jefferies HB, Reinhard C, Kozma SC and Thomas G (1994) Rapamycin selectively represses translation of the "polypyrimidine tract" mRNA family. *Proc Natl Acad Sci USA*. **91**: 4441-4445.

Kabeya Y, Mizushima N, Ueno T, Yamamoto A, Kirisako T, Noda T, Kominami E, Ohsumi Y and Yoshimori T (2000) LC3, a mammalian homologue of yeast Apg8p, is localized in autophagosome membranes after processing. *Embo J* **19**: 5720-5728.

Kanazawa T, Taneike I, Akaishi R, Yoshizawa F, Furuya N, Fujimura S and Kadowaki M (2004) Amino acids and insulin control autophagic proteolysis through different signaling pathways in relation to mTOR in isolated rat hepatocytes. *J Biol Chem*. **279**: 8452-8459.

Kouroku Y, Fujita E, Tanida I, Ueno T, Isoai A, Kumagai H, Ogawa S, Kaufman RJ, Kominami E and Momoi T (2007) ER stress (PERK/eIF α phosphorylation) mediates the polyglutamine-induced LC3 conversion, an essential step for autophagy formation. *Cell Death Differ*. **14**: 230-239.

Kovacs AL and Seglen PO (1981) Inhibition of hepatocytic protein degradation by methylaminopurines and inhibitors of protein synthesis. *Biochim Biophys Acta* **676**: 213-220.

Lawrence BP and Brown WJ (1993) Inhibition of protein synthesis separates autophagic sequestration from the delivery of lysosomal enzymes. *J Cell Sci*. **105**: 473-480.

Machida Y, Okada T, Kurosawa M, Oyama F, Ozawa K and Nukina N (2006) rAAV-mediated shRNA ameliorated neuropathology in Huntington disease model mouse. *Biochem Biophys Res Commun.* **343**: 190-197.

Mizushima N, Yamamoto A, Hatano M, Kobayashi Y, Kabeya Y, Suzuki K, Tokuhiya T, Ohsumi Y and Yoshimori T (2001) Dissection of autophagosome formation using Apg5-deficient mouse embryonic stem cells. *J Cell Biol* **152**: 657-668.

Muchowski PJ and Wacker JL (2005) Modulation of neurodegeneration by molecular chaperones. *Nat Rev Neurosci.* **6**: 11-22.

Nobukuni T and Thomas G (2004) The mTOR/S6K signalling pathway: the role of the TSC1/2 tumour suppressor complex and the proto-oncogene Rheb. *Novartis Found Symp* **262**.

Perutz MF and Windle AH (2001) Cause of neural death in neurodegenerative diseases attributable to expansion of glutamine repeats. *Nature.* **412**: 143-144.

Prick T, Thumm M, Haussinger D and Vom Dahl S (2006) Deletion of HOG1 Leads to Osmosensitivity in Starvation-Induced, but not Rapamycin-Dependent Atg8 Degradation and Proteolysis: Further Evidence for Different Regulatory Mechanisms in Yeast Autophagy. *Autophagy.* **2**: 241-243.

Ross CA and Poirier MA (2004) Protein aggregation and neurodegenerative disease. *Nat Med.* **10**: S10-17.

Ravikumar B, Duden R and Rubinsztein DC. (2002) Aggregate-prone proteins with polyglutamine and polyalanine expansions are degraded by autophagy. *Hum Mol Genet.* **11**(9): 1107-17.

Ravikumar B, Vacher C, Berger Z, Davies JE, Luo S, Oroz LG, Scaravilli F, Easton DF, Duden R, O'Kane CJ and Rubinsztein DC (2004) Inhibition of mTOR induces autophagy and reduces toxicity of polyglutamine expansions in fly and mouse models of Huntington disease. *Nat Genet* **36**: 585-595.

Rubinsztein DC (2006) The roles of intracellular protein-degradation pathways in neurodegeneration. *Nature* **443**: 780-786.

Sabbatini DM (2006) mTOR and cancer: insights into a complex relationship. *Nat Rev Cancer* **6**: 729-734.

Sarkar S, Perlstein EO, Imarisio S, Pineau S, Cordenier A, Maglathlin RL, Webster JA, Lewis TA, O'Kane CJ, Schreiber SL, Rubinsztein DC (2007) Small molecules enhance autophagy and reduce toxicity in Huntington's disease models. *Nat Chem Biol* **3**(6): 331-8.

Scherzinger E, Sittler A, Schweiger K, Heiser V, Lurz R, Hasenbank R, Bates GP, Lehrach H and Wanker EE (1999) Self-assembly of polyglutamine-containing huntingtin fragments into amyloid-like fibrils: implications for Huntington's disease pathology. *Proc Natl Acad Sci U S A.* **96**: 4604-4609.

Shibata M, Lu T, Furuya T, Degtarev A, Mizushima N, Yoshimori T, MacDonald M, Yankner B and Yuan J (2006) Regulation of intracellular accumulation of mutant Huntingtin by Beclin 1. *J Biol Chem* **281**: 14474-14485.

Shintani T and Klionsky DJ (2004) Autophagy in health and disease: a double-edged sword. *Science.* **306**: 990-995.

Tanida I, Ueno T and Kominami E (2004) LC3 conjugation system in mammalian autophagy. *Int J Biochem Cell Biol.* **36**: 2503-2518.

Terada N, Patel HR, Takase K, Kohno K, Nairn AC and Gelfand EW (1994) Rapamycin selectively inhibits translation of mRNAs encoding elongation factors and ribosomal proteins. *Proc Natl Acad Sci U S A.* **91**: 11477-11481.

Waelter S, Boeddrich A, Lurz R, Scherzinger E, Lueder G, Lehrach H, Wanker EE (2001) Accumulation of mutant huntingtin fragments in aggresome-like inclusion bodies as a results of insufficient protein degradation. *Mol Biol Cell* **12**(5): 1393-407.

Wang YL, Liu W, Wada E, Murata M, Wada K and Kanazawa I (2005) Clinico-pathological rescue of a model mouse of Huntington's disease by siRNA. *Neurosci Res.* **53**: 241-249.

Wanker EE, Scherzinger E, Heiser V, Sittler A, Eickhoff H and Lehrach H (1999) Membrane filter assay for detection of amyloid-like polyglutamine-containing protein aggregates. *Methods Enzymol* **309**: 375-386.

Wullschleger S, Loewith R and Hall MN (2006) TOR signaling in growth and metabolism. *Cell.* **124**: 471-484.

Wytenbach A, Swartz J, Kita H, Thykjaer T, Carmichael J, Bradley J, Brown R, Maxwell M, Schapira A, Orntoft TF, Kato K and Rubinsztein DC (2001) Polyglutamine expansions cause decreased CRE-mediated transcription and early gene expression changes prior to cell death in an inducible cell model of Huntington's disease. *Hum Mol Genet* **10**: 1829-1845.

Yamamoto A, Cremona ML and Rothman JE. (2006) Autophagy-mediated clearance of huntingtin aggregates triggered by the insulin-signaling pathway. *J Cell Biol.***172**: 719-731.

Footnotes

Financial Support

This study was supported by the Wellcome Trust prior to October 2006 (MAK, AMT), the Hereditary Disease Foundation (FH), and the Medical Research Council (AW, SH).

Reprints

Andreas Wytenbach, Neuroscience Group, School of Biological Sciences, University of Southampton, Bassett Crescent East, Southampton SO16 7PX, UK

Figure legends

Fig. 1. Atg5^{+/+} and Atg5^{-/-} MEF cells form inclusion bodies containing Ex1HttQ97-EGFP protein but Ex1HttQ25-EGFP is soluble in both cell types. Fluorescent images of Atg5^{+/+} (A) and Atg5^{-/-} (B) MEFs expressing Ex1HttQ25-EGFP or Ex1HttQ97-EGFP 24 h after transfection. Right hand column shows cells co-expressing mRFP-LC3. Nuclei (blue) were stained with Hoechst 33342. Cells expressing Ex1HttQ25-EGFP do not form inclusion bodies (IBs) and show a homogenous expression (left column, green) while Ex1HttQ97-EGFP expressing cells form nuclear (white arrows, middle column) and cytoplasmic IBs (right hand column). Note the absence of DNA where a nuclear IB has been deposited (arrow). Only Atg5^{+/+} cells co-expressing Ex1HttQ97-EGFP and mRFP-LC3 (red) show LC3 punctation (right column, arrowhead). No localisation of mRFP-LC3 to IBs was observed.

Fig. 2. Atg5^{-/-} cells show an increase in the formation of inclusion bodies and SDS-insoluble Ex1HttQ97-EGFP protein. A) The percentage of IBs formed per GFP-positive cells was scored after 1 or 2 days of transfection. Atg5^{-/-} cells form IBs at about 2-fold the rate of Atg5^{+/+} cells up to 2 days post-transfection (mean \pm SD, day 1 n=11, day 2 n=3; $p=1.7 \times 10^{-6}$ by ANOVA, comparisons by t-test, 1 d Atg5^{+/+} vs Atg5^{-/-} $p < 0.0001$, 2 d Atg5^{+/+} vs Atg5^{-/-} $p < 0.02$). B) Left panel: Dot blots of SDS-insoluble extracts generated using the filter-trap assay (see Methods) probed with anti-EGFP. 1x and 0.5x indicate the relative amount of pellet input. Right panel: Respective soluble extracts probed for GFP (top), tERKs (2nd row, a loading control), or LC3 I and II (3rd row). Sample loading for SDS-PAGE and filter trap assays was normalised to protein content. C) MEFs were treated with 50 nM bafilomycin A1 (BafA1) for 20 h after transfection with Ex1HttQ97-EGFP (C = control, no drug treatment) and blots containing equal amounts of soluble protein were probed for LC3I/II, tERKs (loading control) and SDS-insoluble Ex1HttQ97 (dot blot). The amount of LC3 II increased markedly when Atg5^{+/+} cells were incubated in the presence of BafA1, while no LC3 II was detected in Atg5^{-/-} cells. D) Quantification of SDS-insoluble Ex1HttQ97 in Atg5^{+/+} and Atg5^{-/-} cells (mean \pm SD, n=4; no significant differences between Atg5^{-/-} control, Atg5^{-/-}-BafA1 and Atg5^{+/+} BafA1 conditions by ANOVA, $p=0.7$ but $p < 0.001$ between the wt control value and the other three treatments, Tukey's HSD). No insoluble material was obtained from either class of MEF cell transfected with Ex1HttQ25-EGFP.

Fig. 3. Co-localisation of LAMP1, ubiquitin, and vimentin with IBs. Atg^{+/+} or Atg^{-/-} cells were transfected with a construct expressing Ex1HttQ97-EGFP and stained with an anti-ubiquitin antibody (Ubi) and an anti-lysosome-associated membrane protein antibody (Lamp1). A separate set of cells was stained with anti-vimentin. In both Atg^{5+/+} and Atg^{5-/-} cells, ubiquitin, LAMP1 and vimentin redistribute towards inclusion bodies formed by Ex1HttQ97-EGFP in ~5% of the cells, showing that IBs appear to be qualitatively similar.

Fig. 4. Pre-treatment with rapamycin reduces IB load similarly in both Atg^{5+/+} and Atg^{5-/-} MEFs without affecting toxicity, transfection efficiency or nuclear distribution of IBs. MEFs were seeded and allowed to attach before culturing in the presence or absence of 200 nM rapamycin overnight (12 h) after which MEFs were transfected with either Ex1HttQ25-EGFP or Ex1HttQ97-EGFP and cultured for a further 20-24 h without treatment or in the presence of 200 nM rapamycin before extraction. A) Immunoblot of soluble fraction of extracts (see methods for explanation of soluble versus insoluble) normalised to equal protein input. Blots were probed for GFP (top row), tERK (loading control), phospho-serine(235/6)S6, or LC3. No differences were observed in the levels of soluble Ex1HttQ25/97, tERK or LC3 in response to rapamycin treatment, however the reduction in S6 phosphorylation shows that mTOR inhibition was achieved. This experiment was repeated 4 times with similar results. B) The percentage of IBs formed per GFP-positive cells was scored after 1 day (mean ± SD, n=11 (control) or n=10 (rapamycin); ANOVA, p=5x10⁻⁶, Tukey's posthoc: Atg^{5+/+} untreated vs rapamycin p=0.03, Atg^{5-/-} untreated vs rapamycin p=0.003). C) Toxicity was determined by scoring abnormal nuclear morphology using Hoechst 33342. (mean ± SD, n=3, ANOVA p=0.32). D) Efficiency of transfection was scored by counting the present of EGFP-positive cells (mean ± SD, n=3, ANOVA p=0.69). E) Percent of EGFP-positive cells containing nuclear IB was determined by analysing fluorescent images (mean ± SD, n=3, ANOVA p=0.95).

Fig. 5. Pre-treatment with rapamycin reduces SDS-insoluble Ex1HttQ97-EGFP in both Atg^{5+/+} and Atg^{5-/-} MEFs. MEFs were seeded and allowed to attach before culturing in the absence or presence of 200 nM rapamycin overnight (-12 h) after which cells were transfected with Ex1HttQ97-EGFP and cultured for a further 20-24 h. Sample labelled Rap 0 h indicates cells to which rapamycin was added at the time of transfection, and maintained during the subsequent 24 h of culture. The SDS-insoluble fraction of the cells were analysed by filter-trap assay or after resolubilisation with formic acid. A) Representative example of results from filter trap assay (n=3) or formic acid resolubilisation

assay (n=1). B) Percent change in SDS-insoluble material induced by rapamycin (mean \pm SEM, n=6; p<0.05 for the 12 h pre-treatment with rapamycin (-12 h) compared to rapamycin added at zero time (Rap, 0). See Supplementary Fig. S2 for complete data and statistics. Samples used for the filter-trap assay were probed for histone levels, confirming equal loading (data not shown).

Fig. 6. Rapamycin reduces the amount of protein synthesised per cell. A) Atg5^{+/+} and Atg5^{-/-} MEF cultures were plated for 12 h in the absence or presence of 200 nM rapamycin after which two cohorts from each group were transfected with Ex1HttQ25-EGFP or Ex1HttQ97-EGFP and left in the respective media for 24 h. One set of cells was trypsinised and counted to determine cell number (left panel), while total soluble protein was extracted for the other set and the amount of total soluble protein was determined (2nd panel from left). The 3rd panel shows the calculated protein/per cell. Results are depicted as the percentage change between rapamycin-treatment and control. Both cell number and the amount of protein was reduced by rapamycin, leading to a 17% reduction in protein per cell irrespective of expression of the polyQ proteins. Data show mean \pm SD, Q97, n=5, Q25, n=2, untransfected n=3; cell count ANOVA p=0.83; Total soluble protein ANOVA p=0.08; pooled results show that there are no significant differences between the two genotypes, p \geq 0.2). See Supplementary Fig. S3 for complete data and statistics. B) Cells were pretreated with rapamycin and transfected with Ex1HttQ25-EGFP as in (A); the amount of Q25-EGFP/cell was determined by measuring the amount of Q25-EGFP by immunoblotting with an anti-GFP antibody, with the loading normalised to cell number rather than to total protein. Results show mean \pm range from two independent experiments (t-test p=0.7) and demonstrate that rapamycin also reduces protein expression from the plasmid. C) [³⁵S]methionine was added to Atg5^{+/+} cells 30 h after addition of rapamycin and total methionine incorporation was determined after 1 h as detailed in Materials and Methods (mean \pm SD, n=3, t-test p=0.001). D) the percentage change induced by rapamycin is shown alongside the total amount of protein, which was measured, in parallel samples. The third bar shows that the ratio of methionine incorporation to total protein is no different from zero, demonstrating that inhibition of translation is the likely cause of the reduction in the amount of protein/cell.

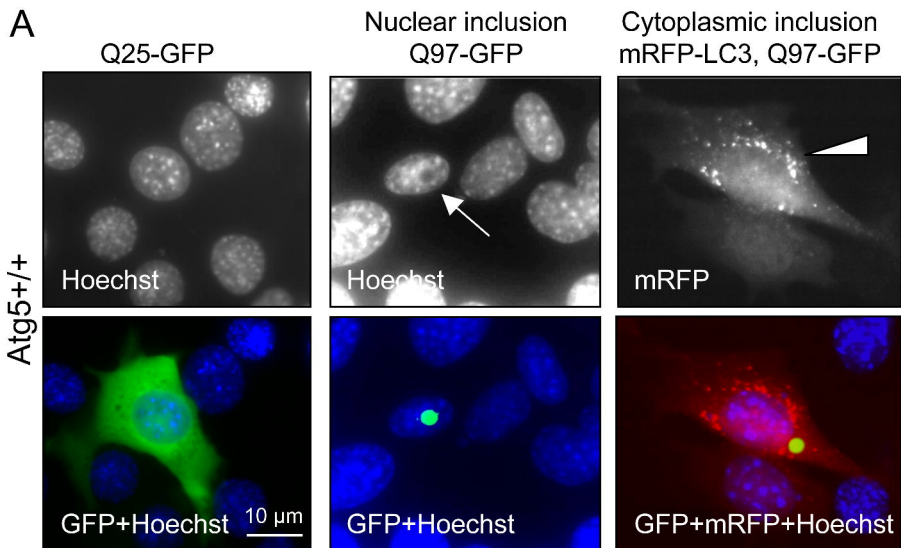
Fig. 7. The reduction in inclusion bodies and insoluble Ex1HttQ97-EGFP induced by rapamycin is mimicked with cycloheximide. Atg5^{+/+} and Atg5^{-/-} MEFs were either pre-treated with rapamycin for 12 h or left untreated before transfection with Ex1HttQ97-EGFP. Cells were then cultured with

rapamycin or cycloheximide (CHX, 0.01 to 0.3 $\mu\text{g/ml}$) for 20 h before protein extraction. A) The soluble fraction was analysed by immunoblotting for GFP, tERK, or phospho-serine235/6-S6 while the insoluble fraction was analysed by filter trap assay for presence of Ex1HttQ97-EGFP. The data below the dot blot show mean \pm range of values from 2 independent experiments. B) EGFP+ve cells were scored for IB. C) [^{35}S]methionine was added to parallel cultures to those described in (A) at the end of the incubation period and the amount of [^{35}S]methionine incorporated was measured after 1 h (mean \pm range, duplicate sample from 2 independent experiments). Cycloheximide treatment caused a similar, dose-dependant decrease in IBs and SDS-insoluble Ex1HttQ97-EGFP in both Atg5 $^{+/+}$ and Atg5 $^{-/-}$ cells, without affecting soluble levels of Ex1HttQ97-EGFP (A, B). Note similarity between the effect of rapamycin (200 nM), and the reduction caused by 0.02-0.1 $\mu\text{g/ml}$ CHX.

Fig. 8. Atg5 over-expression restores autophagic activity in Atg5 $^{-/-}$ cells, reduces SDS-insoluble Ex1HttQ97-EGFP and IB load. Atg5 $^{+/+}$ and Atg5 $^{-/-}$ MEFs were co-transfected with pcDNA3 or pcDNA3ATG5 and either Ex1HttQ25-EGFP or Ex1HttQ97-EGFP at a ratio of 3:1 and cultured for 24 to 96 h. A) After 48 h of Atg5 expression, the soluble fraction was analysed by immunoblotting for Ex1HttQ25-EGFP or Ex1HttQ97-EGFP, Atg5, Atg5/12 conjugate and LC3 I/II. Note that LC3 I processing to LC3 II (and formation of Atg5/12 conjugate) was restored in Atg5 $^{-/-}$ MEFs. B) Atg5 $^{+/+}$ and Atg5 $^{-/-}$ MEFs were co-transfected with pcDNA3 or pcDNA3ATG5 and Ex1HttQ97-EGFP at a ratio of 3:1 and cultured for 24 to 96 h. The blot shows an example of changes in SDS-insoluble material analysed by the filter trap assay over 4 days showing decreased amounts of Ex1HttQ97-EGFP in Atg5 $^{-/-}$ cells re-expressing Atg5. Loading of the dot blot was normalised for each condition (30 μg of protein). C) Cells expressing Atg5 for 1 day were analysed for SDS-insoluble Ex1HttQ97-EGFP. (mean \pm SEM, n=4, p<0.02, t test). D) Cells were split day 2 after transfection (so that they could be analysed for 2 more days without overcrowding) and the amount of insoluble HttEx1Q97-EGFP was quantified at day 2, 3 and 4. Because of varying concentrations of cells between the different experiments, the data were normalised to the values obtained at day 2. Note the increased rate of reduction in insoluble HttEx1Q97-EGFP in Atg5 $^{-/-}$ cells expressing Atg5 compared to untransfected Atg5 $^{-/-}$ cells and the lack of effect of Atg5 overexpression in the Atg5 $^{+/+}$ cells in panels C and D.

Figure 1

A



B

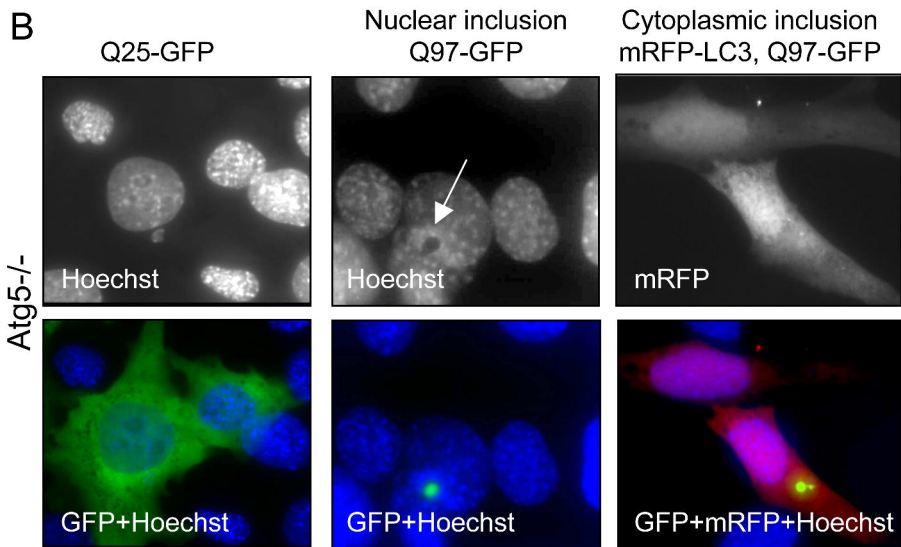


Figure 2

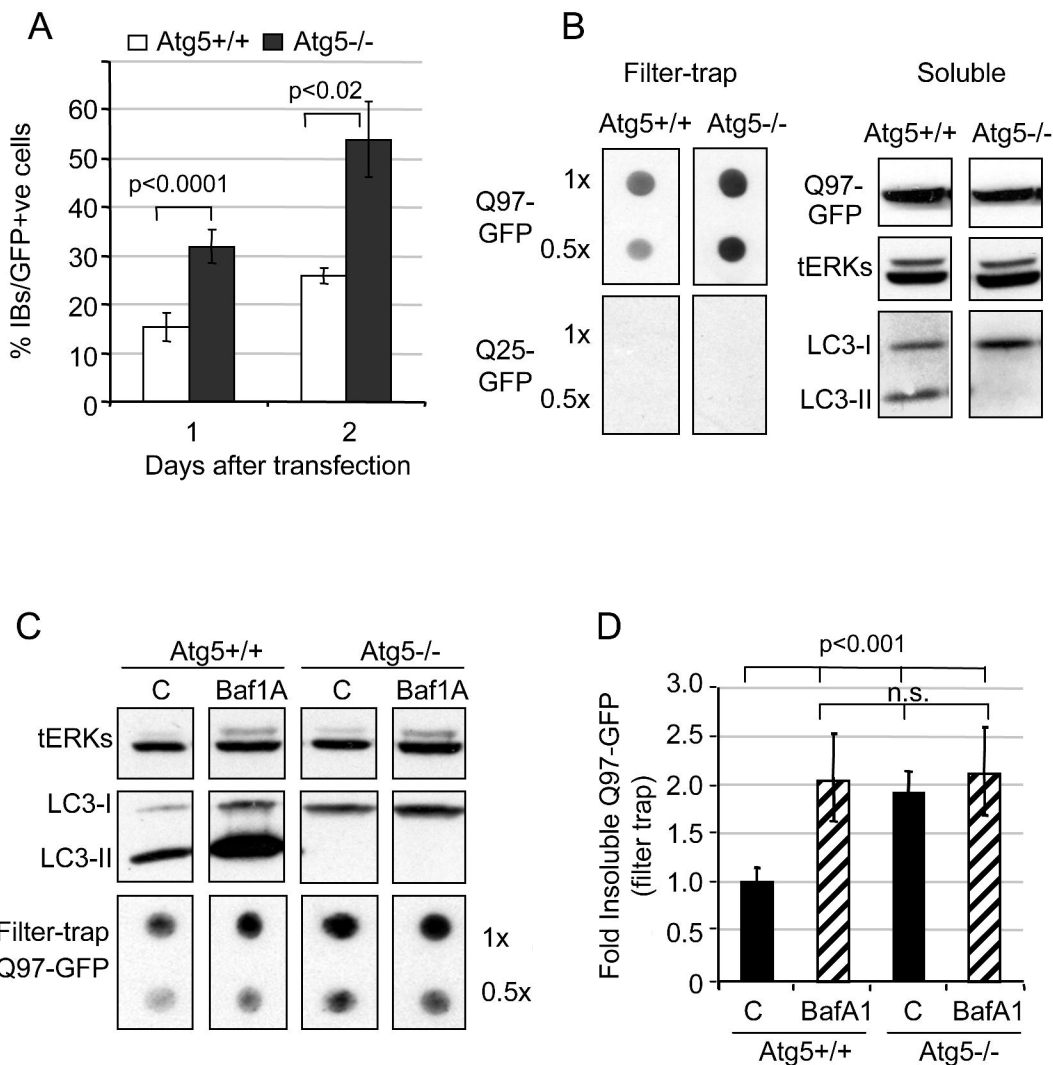


Figure 3

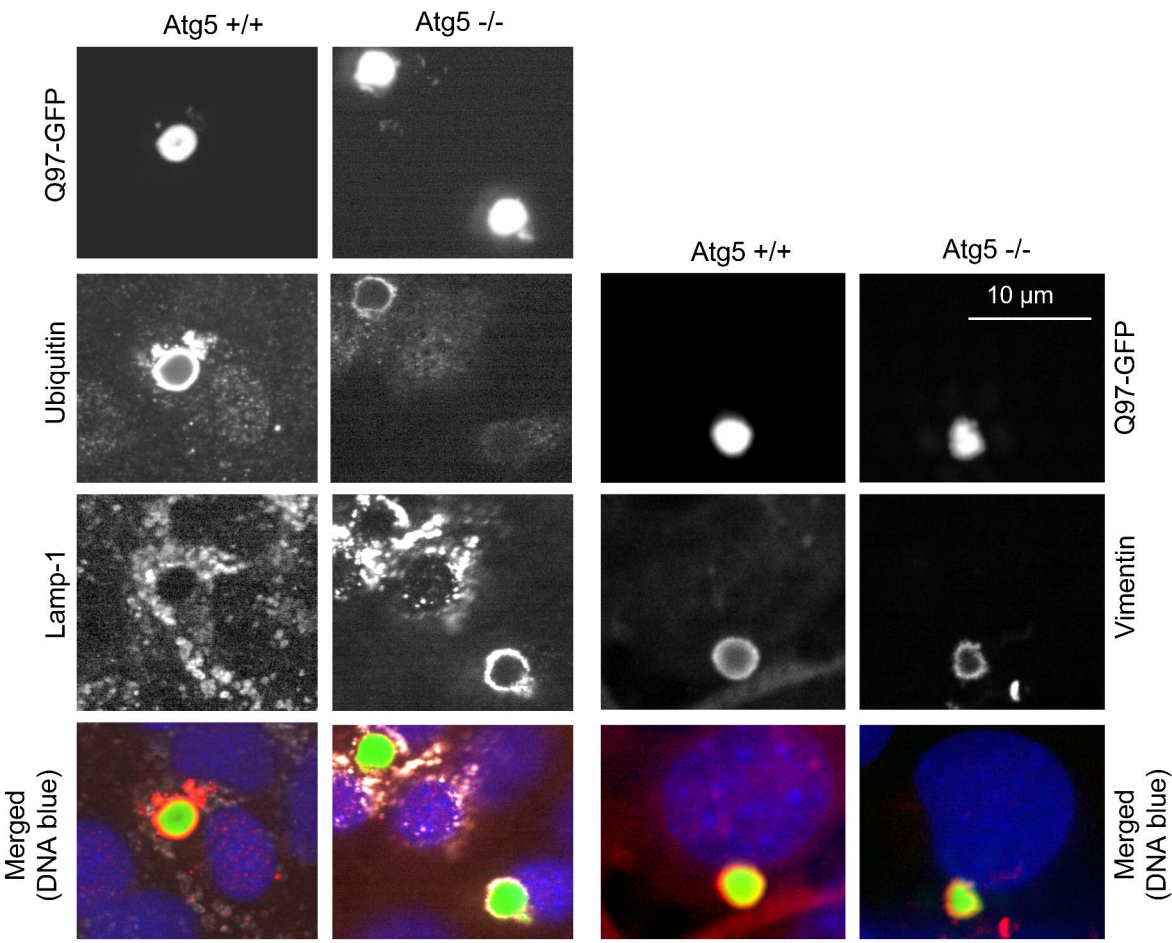


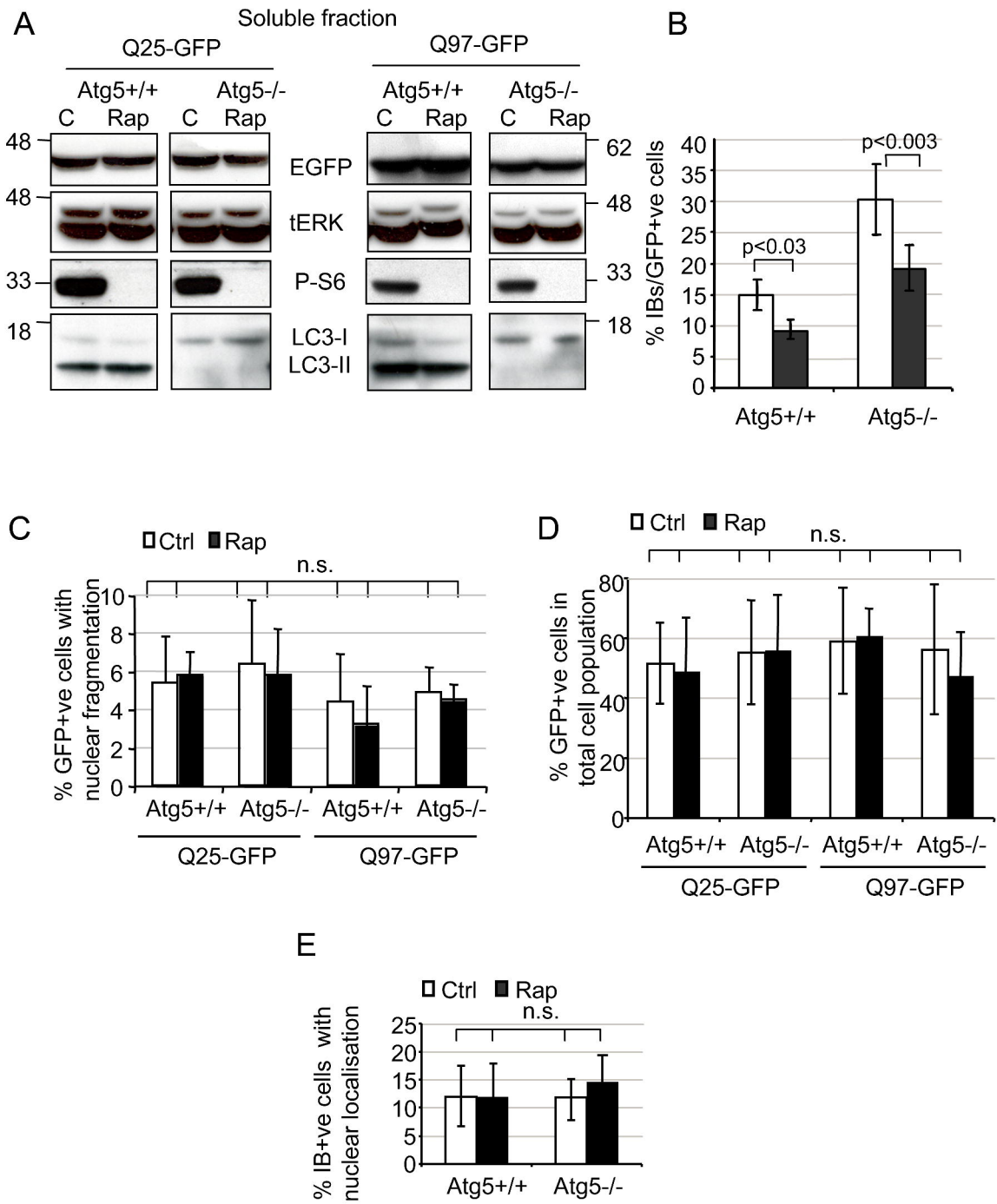
Figure 4

Figure 5

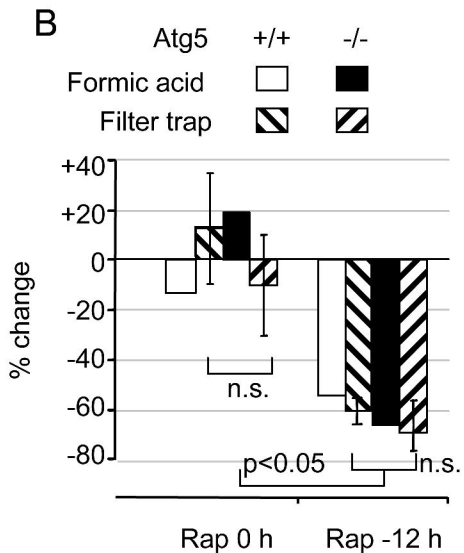
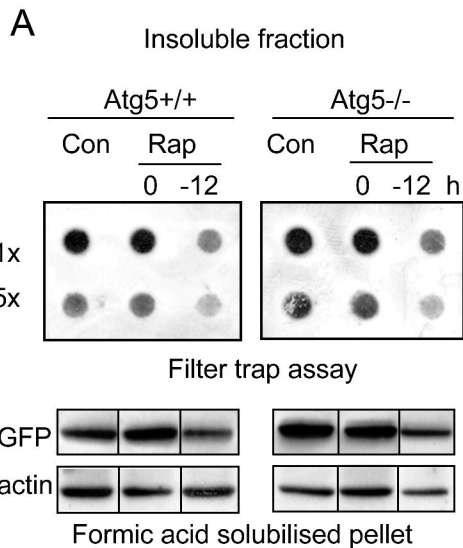


Figure 6

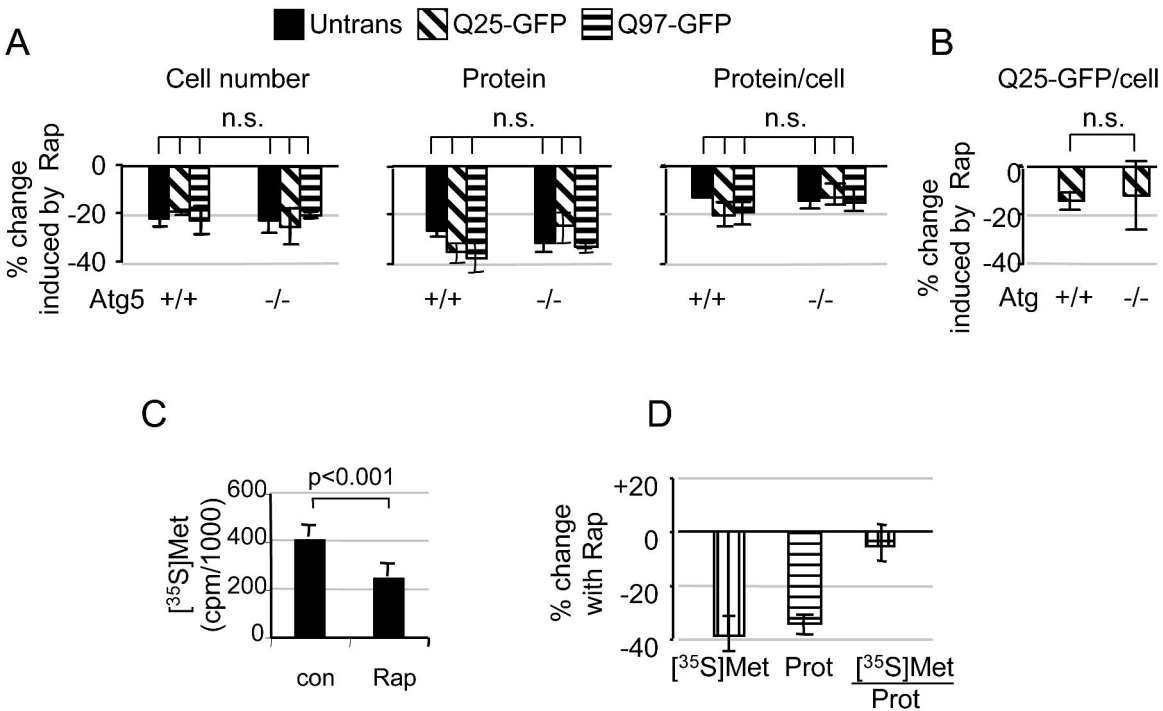


Figure 7

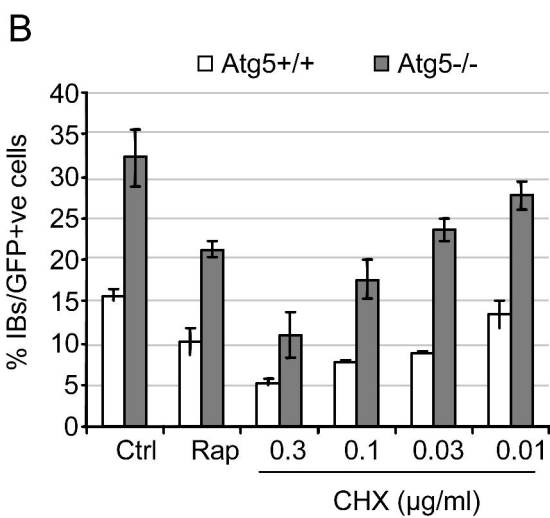
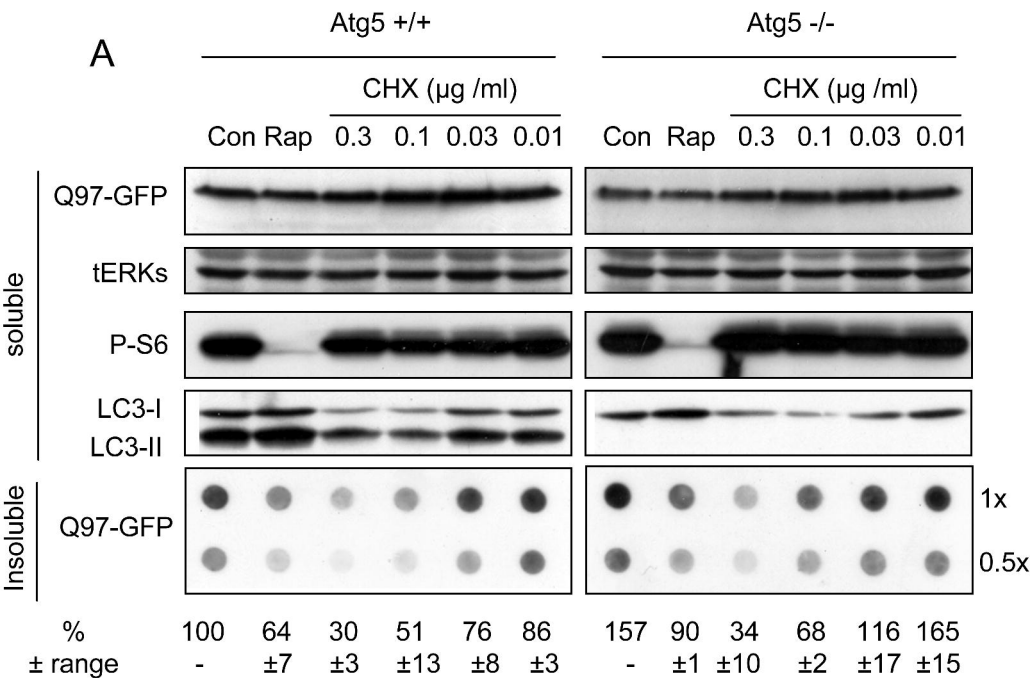


Figure 8

